

Effect of a Trailing-Edge Jet on Fin Buffeting

S. Phillips,* C. Lambert,† and I. Gursul‡

University of Bath, Bath, England BA2 7AY, United Kingdom

Effect of a trailing-edge jet on the interaction of a leading-edge vortex with a fin and resulting fin buffeting was investigated in water-tunnel as well as wind-tunnel experiments. Flow visualization showed that fin-induced vortex breakdown can be delayed into the wake even for the head-on collision of the leading-edge vortex with the fin. Hence it was demonstrated that the adverse pressure gradient caused by the presence of the fin could be overcome with a deflected trailing-edge jet. Delay of vortex breakdown into the wake even for relatively small values of jet velocity ratio is possible for deflected jets, whereas the effectiveness of the jet with no deflection is very limited. Buffeting response of a flexible fin in wind-tunnel experiments showed that there was considerable delay of the onset of buffeting to higher angles of attack with increasing jet momentum for $\beta = 30$ and 45 deg. Depending on the fin location with respect to the leading-edge vortex, it was possible to shift the buffeting envelope as much as 12 deg in incidence of the wing. Experiments with varying wing sweep angle showed that jet blowing was as effective in attenuating fin buffeting for less slender wings. Wind-tunnel experiments also showed that the nozzle geometry is very important and causes very different buffeting envelopes for the same momentum coefficient.

Introduction

EXPERIMENTAL evidence suggests that several unsteady flow phenomena can cause fin buffeting. These phenomena and their physical models were recently discussed by Gursul and Xie.¹ However, vortex breakdown phenomenon is the most important source of buffeting over delta wings. A wide variety of investigations was conducted on both simplified fin-delta-wing configurations and fins on actual model aircraft in order to understand the mechanisms of fin buffeting and the relation to the vortical flowfields over the wing.^{2–13} A good summary of the experimental investigations is given by Wolfe et al.⁸

Both structural-control and flow-control methods have been used by previous investigators to attenuate fin buffeting. Structural methods include increasing the stiffness and damping. There have also been attempts to reduce the buffeting with active vibration control techniques using piezoelectric actuators¹⁴ or an active rudder¹⁵ without any knowledge of the flowfield. Unfortunately, only modest reductions in fin response are possible with the structural control methods in the absence of any flow-control method. Regarding flow-control methods, several techniques are available in order to alter the position of the vortex with respect to the fin or delay vortex breakdown. These include blowing¹⁶ and suction¹⁷ on the wing surface, fences,³ and variable position leading-edge extensions.¹⁸ A general review of vortex breakdown control methods is presented by Mitchell and Delery.¹⁹ Common to these investigations was the introduction of modifications well upstream of the breakdown and close to the origin of the vortex. However, these methods are not effective over a wide range of angle of attack encountered during a maneuver because of drastic changes in the position of the vortex. Moreover, the effectiveness of these techniques reaches a saturation with increasing control parameter (such as the blowing coefficient) as one tries to delay the location of vortex breakdown because vortex breakdown phenomenon strongly depends on the external pressure gradient. Trailing edge of the wing and, more importantly, the fin itself produces an adverse pressure gradient, which

is the dominant factor in determining the location of vortex breakdown and the magnitude of fin buffeting. Limited effectiveness of the flow-control techniques just mentioned is caused by incapability of altering the external pressure gradient while modifying the structure of the vortices.

The purpose of this study is to investigate a different aspect of vortex control technique, which is more likely to alter the external pressure gradient, and involves a jet at the trailing edge of the wing. As the beneficial effects of trailing-edge blowing on vortex breakdown over delta wings are well known,^{20–23} this has good potential to overcome the adverse pressure gradient caused by the trailing edge and the fin and to delay vortex breakdown and attenuate fin buffeting. Thrust vectoring remains as a preferred method of integrating propulsive and lift systems for modern fighter aircraft, which can have thrust/weight ratio larger than unity.²⁴ This means that large amount of mass injection through trailing-edge jets is possible. This study concentrates on the effects of a trailing-edge jet on fin buffeting.

Experimental Setup

Water-Tunnel Experiments

Initial experiments with trailing-edge blowing were performed in a water tunnel located in the University of Bath because of its advantages in flow visualization. The water tunnel has a horizontal working section, with a cross-sectional area of 15 by 20 in. (381 by 508 mm). The delta wing and fin were designed and scaled to those used in the wind-tunnel experiments previously reported elsewhere.²⁵ The wing and rigid fin are shown in Fig. 1. The chord length is $c = 250$ mm, giving a Reynolds number around $Re = 2.5 \times 10^4$ for $U_\infty = 10$ cm/s. At the maximum angle of attack $\alpha = 40$ deg, the blockage ratio was 6%, and no correction on the data was attempted. The fin was attached to the trailing edge of the wing with a screw, and the location of the fin could be varied from $y_f/s = 0.0$ to 1.0 with increments of 0.1.

For the trailing-edge blowing experiments a rectangular nozzle with an aspect ratio of 6 and a width of 30 mm was placed underneath the wing as shown in Fig. 1. The centerline of the nozzle coincided with the approximate position of the vortex axis ($y_v/s \approx 0.6$) within the range of angle of attack tested. The spanwise location of the vortex was estimated from the pressure measurements across the span at $x/c = 0.5$ in the absence of the fin.²⁵ It was found that the location of the suction peak is only slightly affected by the angle of attack, showing that the spanwise location of the leading-edge vortex is roughly constant. An important parameter was jet deflection angle β , which was generated by using a thin plate with the same width

Received 16 February 2002; revision received 17 September 2002; accepted for publication 18 September 2002. Copyright © 2003 by the authors. Published by the American Institute of Aeronautics and Astronautics, Inc., with permission. Copies of this paper may be made for personal or internal use, on condition that the copier pay the \$10.00 per-copy fee to the Copyright Clearance Center, Inc., 222 Rosewood Drive, Danvers, MA 01923; include the code 0021-8699/03 \$10.00 in correspondence with the CCC.

*Student, Department of Mechanical Engineering.

†Postgraduate Student, Department of Mechanical Engineering.

‡Reader in Aerospace Engineering, Department of Mechanical Engineering. Member AIAA.

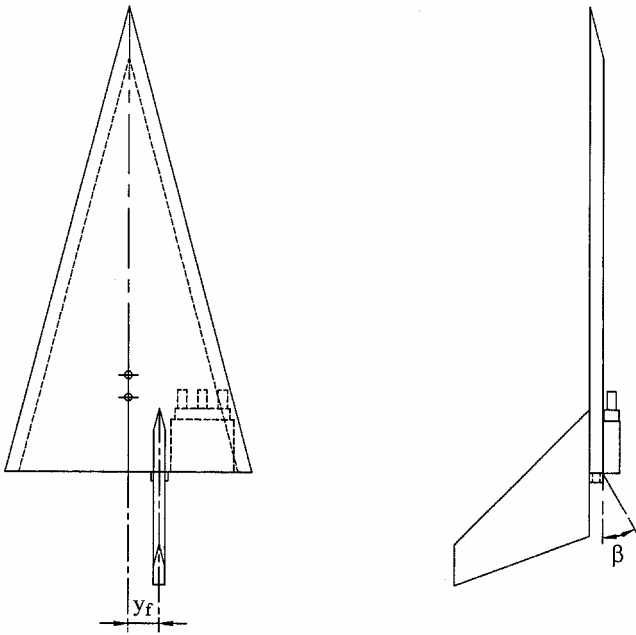


Fig. 1 Definition of fin location y_f and jet deflection angle β .

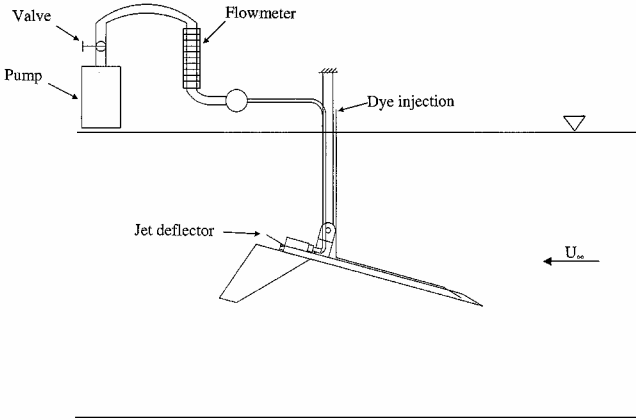


Fig. 2 Schematic of the experimental setup in water tunnel.

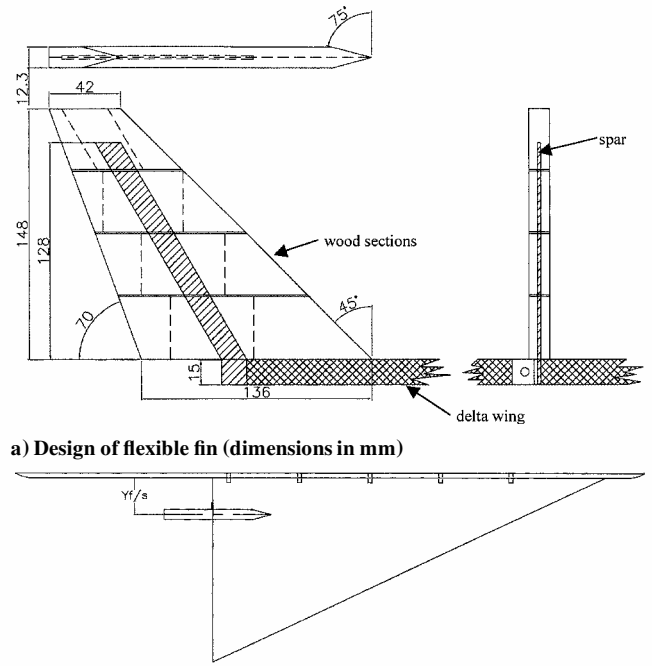
as the nozzle to deflect the jet (see Fig. 1). The volumetric flow rate of the jet was measured by a rotameter, which was placed at the discharge side of a submersible pump as shown in Fig. 2. The maximum jet velocity obtained was $U_{jet}/U_\infty = 8.9$, which corresponds to a momentum coefficient of

$$C_\mu = \rho U_{jet}^2 A_{jet} / \frac{1}{2} \rho U_\infty^2 S_w = 0.708$$

Here A_{jet} and S_w denote cross-sectional area of nozzle exit and surface area of the wing. As the thrust/weight ratio can be larger than unity,²⁴ it can be shown that the momentum coefficient can take up values on the order of unity. The values of the momentum coefficient used in the experiments are therefore realistic and also consistent with the range used by the other investigators.^{20–23} In the water-tunnel experiments dye flow visualization was used to visualize the vortex trajectories and breakdown location. A digital video camera was used to record the flow visualization and to further analyze the results. The measurement uncertainty for vortex breakdown location was 1% of the chord length. Estimated uncertainty for the momentum coefficient was 2%.

Wind-Tunnel Experiments

Additional experiments in a 2.12 by 1.51 m low-speed wind tunnel were carried out to demonstrate the applicability of the proposed control methods at higher Reynolds numbers. A flexible fin shown in Fig. 3a was designed and fabricated. It consists of a thin aluminum spar surrounded by several wood segments to provide aerodynamic



a) Design of flexible fin (dimensions in mm)

b) Half-delta wing modal, fin and splitter plate

Fig. 3 Overview of the experimental setup in wind tunnel.

shaping. The advantages that the wood sections offer are low material density and ease of fabrication. These sections were attached to the spar with small bolts. With this design the contribution of the wood sections to the bending stiffness of the spar is minimized. The dimensions of the spar were chosen to obtain the natural frequencies of the first bending mode for a typical modern combat aircraft. The thickness of the spar was 2 mm. The leading edge of the fin was double bevelled at an angle of 30 deg. The main dimensions of the fin are given in Fig. 3a. The spar was attached to the delta wing by a bracket near the trailing edge of the wing.

The experimental setup, which uses a half-model delta wing and a splitter plate, is shown in Fig. 3b. Three delta-wing models with sweep angles $\Lambda = 65, 70,$ and 75 deg were used in the experiments, although the majority of the tests were carried out for $\Lambda = 75$ deg as in our previous investigations and in water-tunnel experiments. All three wings had a chord length of $c = 500$ mm and a thickness of 15 mm. The lee surface was flat, whereas the leading edges were bevelled at 45 deg on the windward side. The Reynolds number based on the chord length was $Re = 3.5 \times 10^5$. For $\Lambda = 75$ deg the dimensions of the delta wing and fin are scaled to those used in the water-tunnel experiments. Buffeting response of this flexible fin was investigated by measuring the fin vibration levels sensed by a tip accelerometer attached to the spar. The measurement uncertainty for the tip acceleration is estimated as 2%. In addition to calculating the rms value of the fin tip acceleration, the spectra of the tip acceleration were examined for each case. The fin vibrations occurred at the natural frequency of the first bending mode, which is hardly influenced by the angle of attack.

An identical nozzle scaled to one used in the water-tunnel experiments was connected to pressured air supply to produce the trailing-edge jet. The mass flow of the jet was monitored by a rotameter, and the maximum momentum coefficient obtained was $C_\mu = 0.287$ for $\Lambda = 75$ -deg delta wing. Because of the limitations of the air supply, this maximum momentum coefficient was considerably smaller than that used in the water-tunnel experiments.

Results

Water-Tunnel Experiments

Previous wind-tunnel investigation²⁵ using a flexible fin showed that the fin location y_f/s is a very important parameter in addition to the angle of attack. Outboard fin locations produce very light buffeting, surprisingly even at high angle of attack. Inboard fin locations can produce the heaviest buffeting, depending on the angle

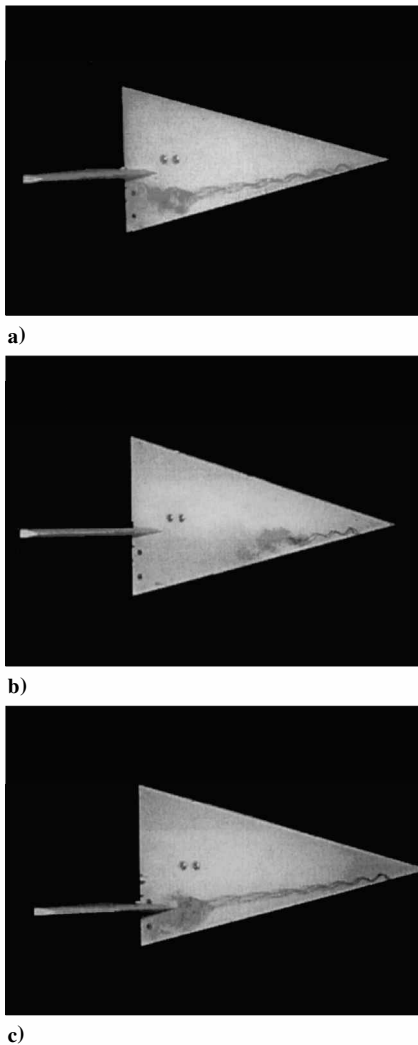


Fig. 4 Flow visualization for a) $y_f/s = 0.2$, $\alpha = 25$ deg; b) $y_f/s = 0.2$, $\alpha = 35$ deg; and c) $y_f/s = 0.6$, $\alpha = 23$ deg for no jet blowing.

of attack. At low to moderate angles of attack, the buffeting is light. An example is shown in Fig. 4a for $y_f/s = 0.2$ and $\alpha = 25$ deg. At high angle of attack, in particular when the shear layer impinges on the fin, the heaviest buffeting is observed. Here, the shear layer refers to the region of large velocity gradient formed between nearly stagnant flow near the center of vortex and the freestream. An example is shown in Fig. 4b for $y_f/s = 0.2$ and $\alpha = 35$ deg. A particularly interesting configuration is for $y_f/s = 0.6$, which corresponds to the approximate position of the vortex axis within the range of angle of attack tested. An example is shown in Fig. 4c for $\alpha = 23$ deg. Because of the adverse pressure gradient produced by the presence of the fin, vortex breakdown is always observed upstream of the fin. This head-on collision of the vortex with the fin produces moderate level of buffeting, when compared to heavy buffeting produced for inboard fin locations. The fact that the head-on collision does not produce large buffeting when the center of the vortex impinges on the fin is consistent with the previous work.^{4,10} Consequently, we focused on the fin locations $y_f/s = 0.2, 0.4$, and 0.6 in this study.

Figures 5–7 show flow visualization pictures for a) no flow control and b) jet blowing at the maximum flow rate ($U_{jet}/U_\infty = 8.9$, $C_\mu = 0.708$) for $y_f/s = 0.2, 0.4$, and 0.6 . The angle of attack is $\alpha = 31$ deg, and the jet deflection angle $\beta = 30$ deg. It is seen that vortex breakdown is delayed into the wake for all three fin locations when the jet is turned on. In fact, even for the head-on collision ($y_f/s = 0.6$) it is possible to eliminate the breakdown completely. Effect of the velocity ratio U_{jet}/U_∞ on the location of vortex breakdown is shown in Fig. 8 for $\alpha = 30$ and 40 deg for various jet deflection angles β . Figure 8a shows that complete elimination of vortex breakdown even for relatively small values of jet velocity

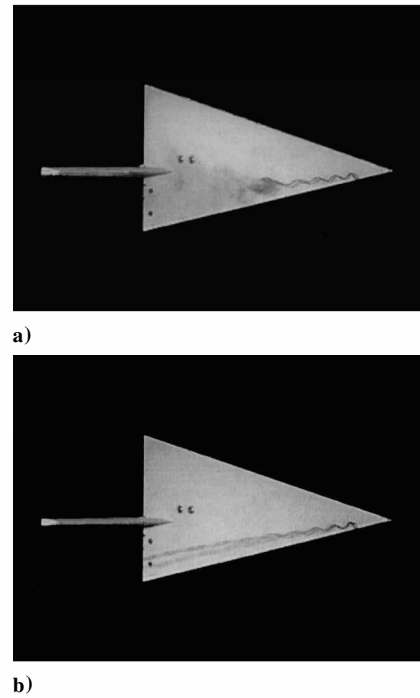


Fig. 5 Flow visualization for $y_f/s = 0.2$, $\alpha = 31$ deg, $\beta = 30$ deg: a) $U_{jet}/U_\infty = 0$ and b) $U_{jet}/U_\infty = 8.9$ ($C_\mu = 0.708$).

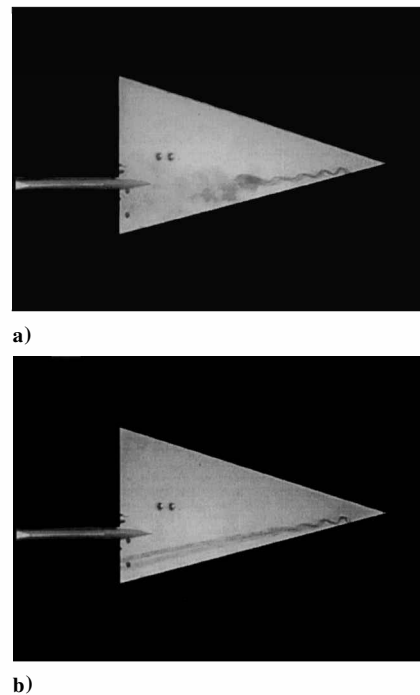
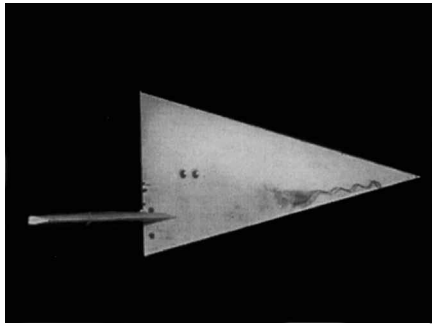
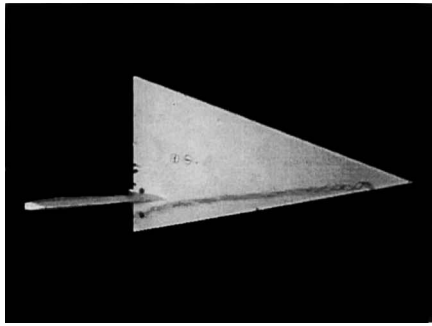


Fig. 6 Flow visualization for $y_f/s = 0.4$, $\alpha = 31$ deg, $\beta = 30$ deg: a) $U_{jet}/U_\infty = 0$ and b) $U_{jet}/U_\infty = 8.9$ ($C_\mu = 0.708$).

ratio is possible for deflected jets, whereas the effectiveness of the jet with no deflection ($\beta = 0$ deg) is very limited. Positive effect of jet deflection in delaying vortex breakdown was noted previously for a delta wing²¹ and with no fin. Our results for $y_f/s = 0.2$ is consistent with those of Ref. 21. Similar observations can be made from Fig. 8b for a higher angle of attack, although flow control is less effective overall. No attempts were made to study the effect of deflection angle in detail, and only four values of β were used in the current experiments. Nevertheless, the results suggest that there might be an optimum value of β , which may depend on the angle of attack. Consequently we performed detailed flow visualization experiments for $\beta = 30$ and 0 deg for comparison.



a)



b)

Fig. 7 Flow visualization for $y_f/s = 0.6$, $\alpha = 31$ deg, $\beta = 30$ deg: a) $U_{jet}/U_\infty = 0$ and b) $U_{jet}/U_\infty = 8.9$ ($C_\mu = 0.708$).

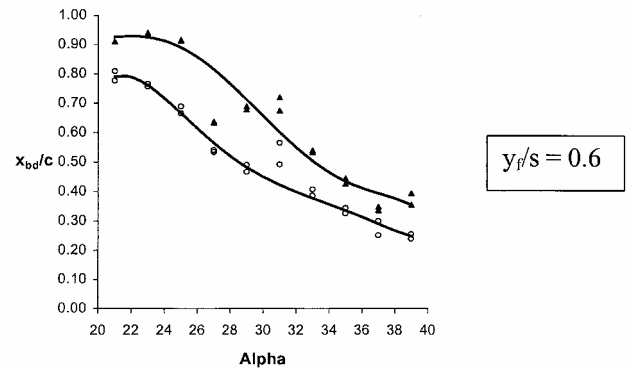
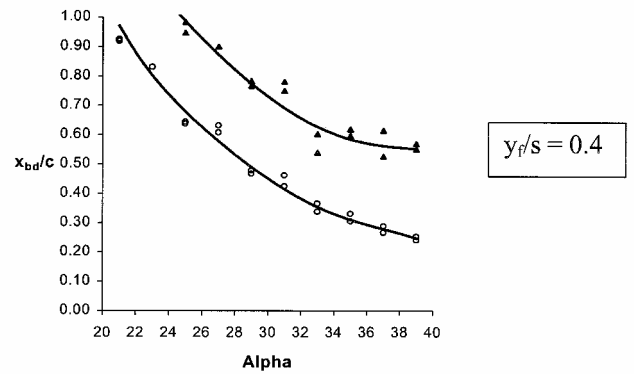
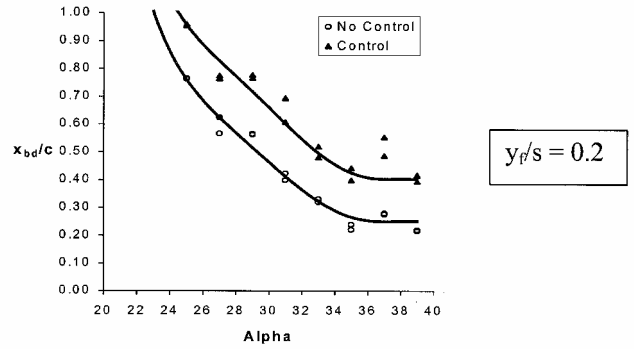
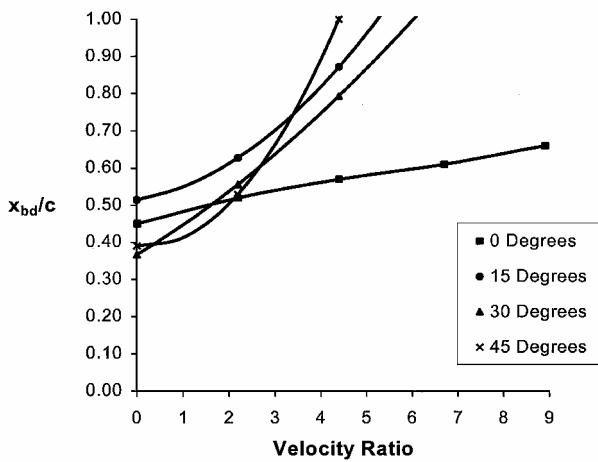
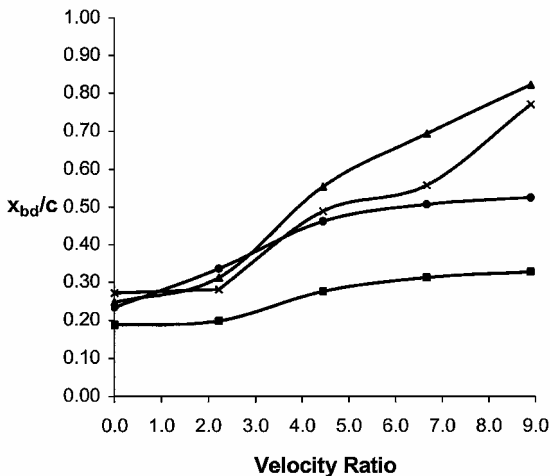


Fig. 9 Variation of breakdown location with angle of attack for $\beta = 0$ deg.



a)



b)

Fig. 8 Variation of vortex breakdown location as a function of velocity ratio for $y_f/s = 0.2$, jet deflection angles $\beta = 0, 15, 30,$ and 45 deg, and for a) $\alpha = 30$ deg and b) $\alpha = 40$ deg.

Figures 9 and 10 show the variation of breakdown location as a function of angle of attack for three fin locations for $\beta = 0$ and 30 deg, respectively. In each case no flow control ($U_{jet}/U_\infty = 0$) and jet blowing at the maximum flow rate ($U_{jet}/U_\infty = 8.9$, $C_\mu = 0.708$) are compared. Each data point represents the time-averaged breakdown location, and large scatter of data is observed, in particular for the jet blowing, which indicates the unsteady character of vortex/jet interaction. It is seen in Fig. 9 that, for $\beta = 0$ deg, vortex breakdown location is delayed 20 to 30% of the chord length with a trailing-edge jet. For $\beta = 30$ deg shown in Fig. 10, the delay is around 40 to 60% of the chord length. For $y_f/s = 0.2$ and 0.4 vortex breakdown can be completely eliminated up to an angle of attack of around 35 deg. Even for the head-on collision case $y_f/s = 0.6$ for which vortex breakdown is always upstream of the fin, breakdown can be eliminated up to $\alpha = 30$ deg with jet blowing. A summary of the results presented in Figs. 9 and 10 is shown in Fig. 11 together with the results for no fin case. It is seen that for $U_{jet}/U_\infty = 0$ breakdown location for all three fin locations is further upstream compared to no fin case, and the effect of fin location is negligible for $x_{bd}/c \leq 0.6$. For $U_{jet}/U_\infty = 8.9$ ($C_\mu = 0.708$) breakdown location for $y_f/s = 0.2, 0.4,$ and no fin case roughly collapse, whereas vortex breakdown for the head-on collision case is further downstream.

The results presented so far show that vortex breakdown caused by the presence of a fin can be completely eliminated by a trailing-edge jet even at high angle of attack. Most likely reason behind this improvement is that the trailing-edge jet creates a favorable pressure

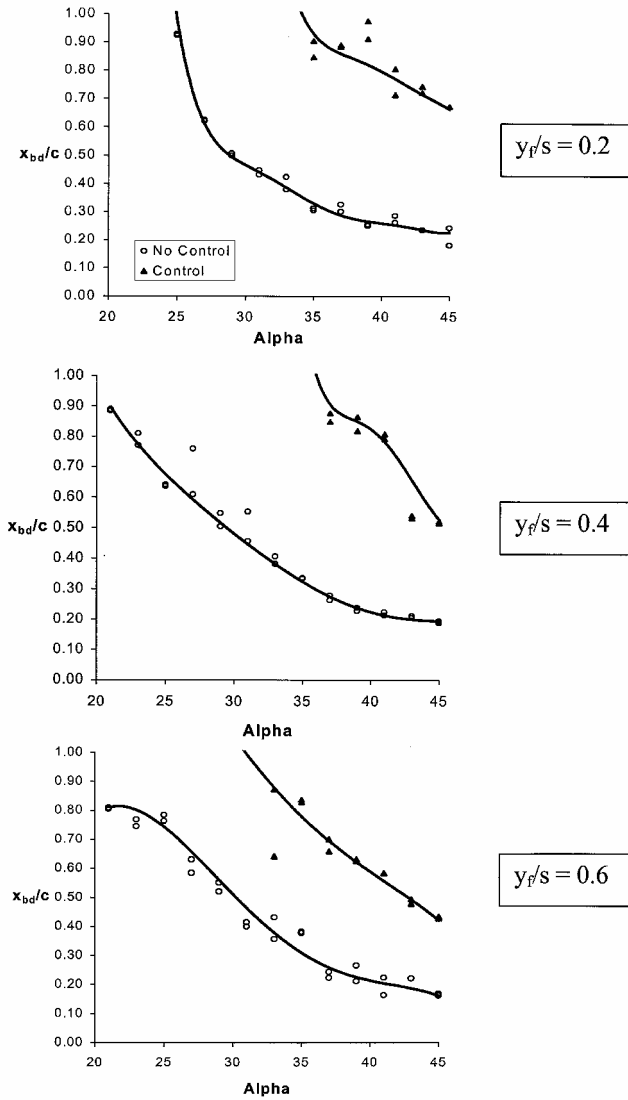


Fig. 10 Variation of breakdown location with angle of attack for $\beta = 30$ deg.

gradient near the trailing edge²¹ and reduces the adverse pressure gradient caused by the fin. This is similar to the early experiments of Lambourne and Bryer,²⁶ who showed that a downward deflection of a trailing-edge flap delayed the vortex breakdown. Likewise, vortex breakdown could be completely eliminated on a cambered delta wing. It can be argued that a deflected jet acts like a deflected flap and accelerates the flow near the trailing edge, and hence reduces the adverse pressure gradient. However, there are other factors such as entrainment effects suggested by Ref. 20 and the interaction between the jet and the wing vortices.²⁷ As the jet exhausts into a crossflow, a counter-rotating vortex pair is generated. Wang et al.²⁷ showed that wing vortices can be drawn toward the jet center by the induced velocity created by the jet vortices. Figures 12 show flow visualization pictures for a) $U_{jet}/U_\infty = 0$, b) $U_{jet}/U_\infty = 8.9$ (in a "steady-state case"), c) right after the jet is turned off, for the following parameters: $y_f/s = 0.2$, $\alpha = 30$ deg, $\beta = 30$ deg. It is seen that the leading-edge vortex is drawn toward the jet and is nearly parallel to the jet in the steady-state case. When the jet is turned off, the wing vortex realigns itself to become nearly parallel to the freestream. Then the vortex breakdown slowly propagates upstream and eventually reaches a steady-state location similar to that shown in Fig. 12a. The role of jet entrainment and jet/vortex interactions deserves further study.

Wind-Tunnel Experiments

To quantify the effect of trailing-edge jet on the buffeting of the flexible fin, detailed experiments were carried out for $\Lambda = 75$ -deg

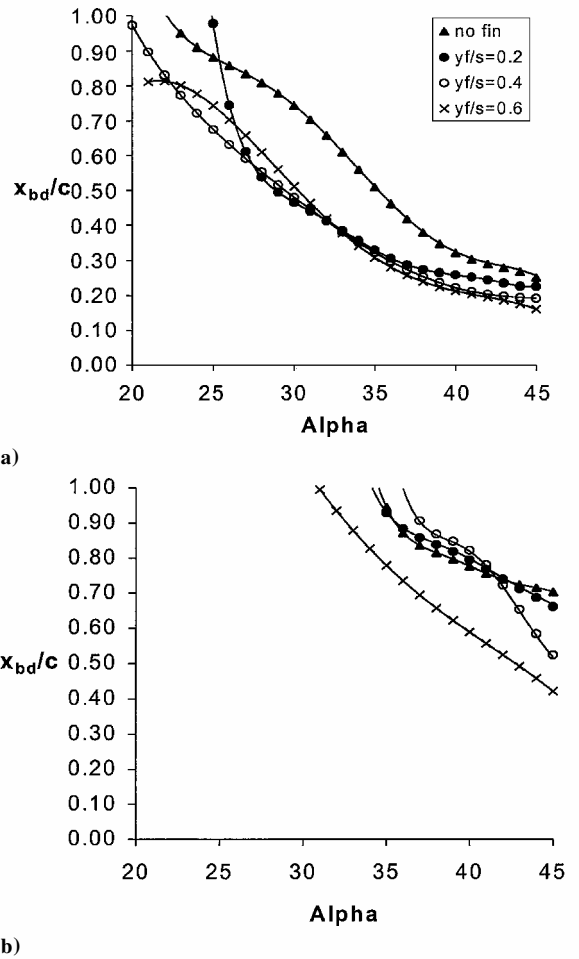


Fig. 11 Variation of breakdown location with angle of attack for $\beta = 30$ deg and a) $U_{jet}/U_\infty = 0$ and b) $U_{jet}/U_\infty = 8.9$ ($C_\mu = 0.708$).

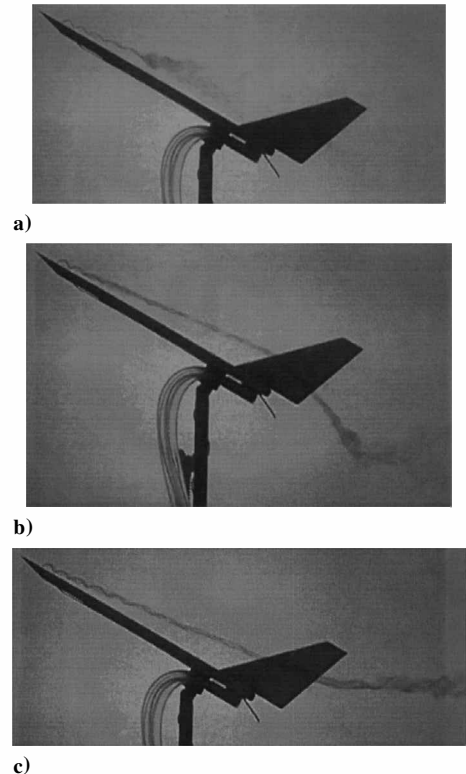


Fig. 12 Flow visualization for a) $U_{jet}/U_\infty = 0$, b) $U_{jet}/U_\infty = 8.9$ ($C_\mu = 0.708$), and c) right after the jet is turned off, $y_f/s = 0.2$, $\alpha = 30$ deg, and $\beta = 30$ deg.

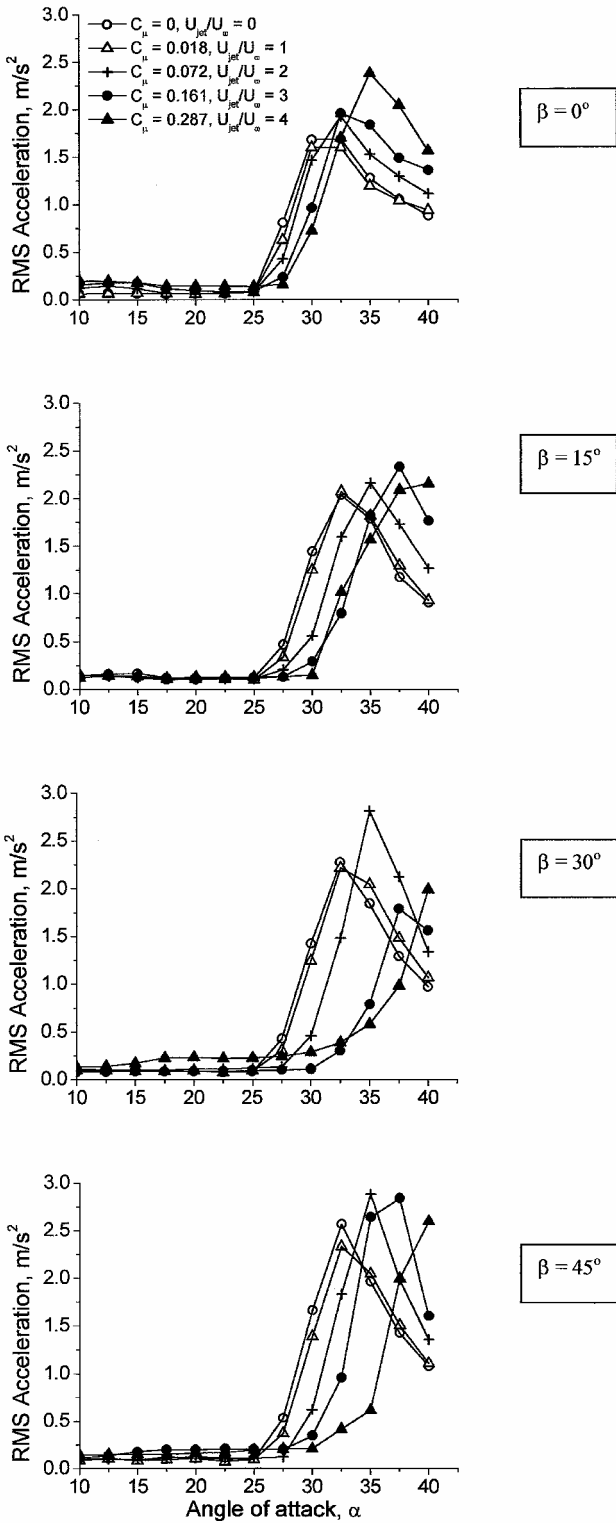


Fig. 13 Variation of rms tip acceleration as a function of incidence for $y_f/s = 0.2$.

delta wing for $y_f/s = 0.2, 0.4, 0.6$, and jet deflection angles $\beta = 0, 15, 30$, and 45 deg. Figure 13 shows the variation of the rms tip acceleration as a function of angle of attack for various momentum coefficients for the fin location $y_f/s = 0.2$. It is seen that the effect of the jet momentum is very small for $\beta = 0$ deg, but there is considerable delay of the onset of buffeting with increasing jet momentum for $\beta = 30$ and 45 deg. It is possible to shift the buffeting envelope as much as 8 deg in angle of attack at the largest momentum coefficient. Hence, blowing at the trailing edge appears to be more effective at the higher jet deflection angles. These results are consistent with the flow visualization pictures obtained in the water

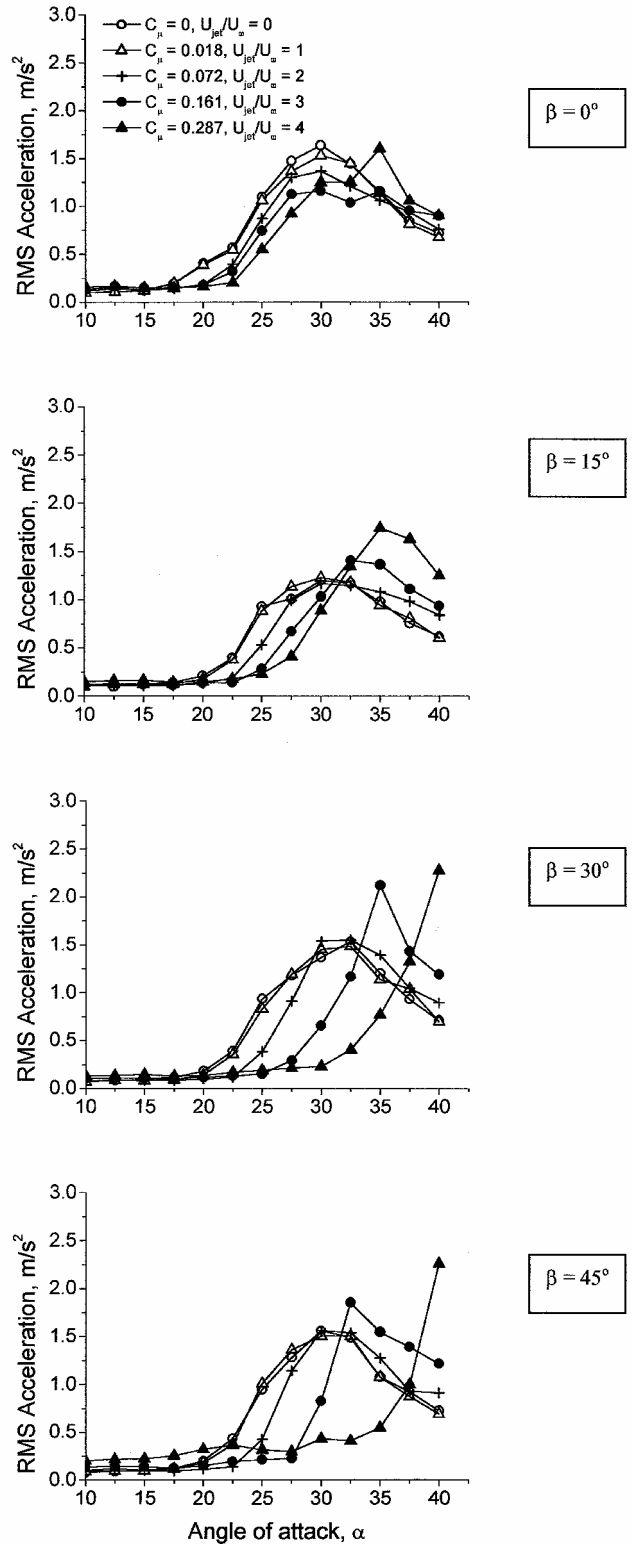


Fig. 14 Variation of rms tip acceleration as a function of incidence for $y_f/s = 0.4$.

tunnel (see Figs. 8–10). Figure 14 shows the variation of the rms tip acceleration as a function of angle of attack for various β and $y_f/s = 0.4$. Again there is negligible effect for $\beta = 0$ deg, whereas delays of as much as 12 deg in the buffeting onset incidence are possible at high jet deflection angles. The results for $y_f/s = 0.2$ and 0.4 are very similar with clear delays in buffeting response to higher angles of attack when the jet is turned on, although the buffeting levels are somewhat smaller for $y_f/s = 0.4$.

Figure 15 shows the variation of the rms tip acceleration as a function of angle of attack for various β and $y_f/s = 0.6$. Note that

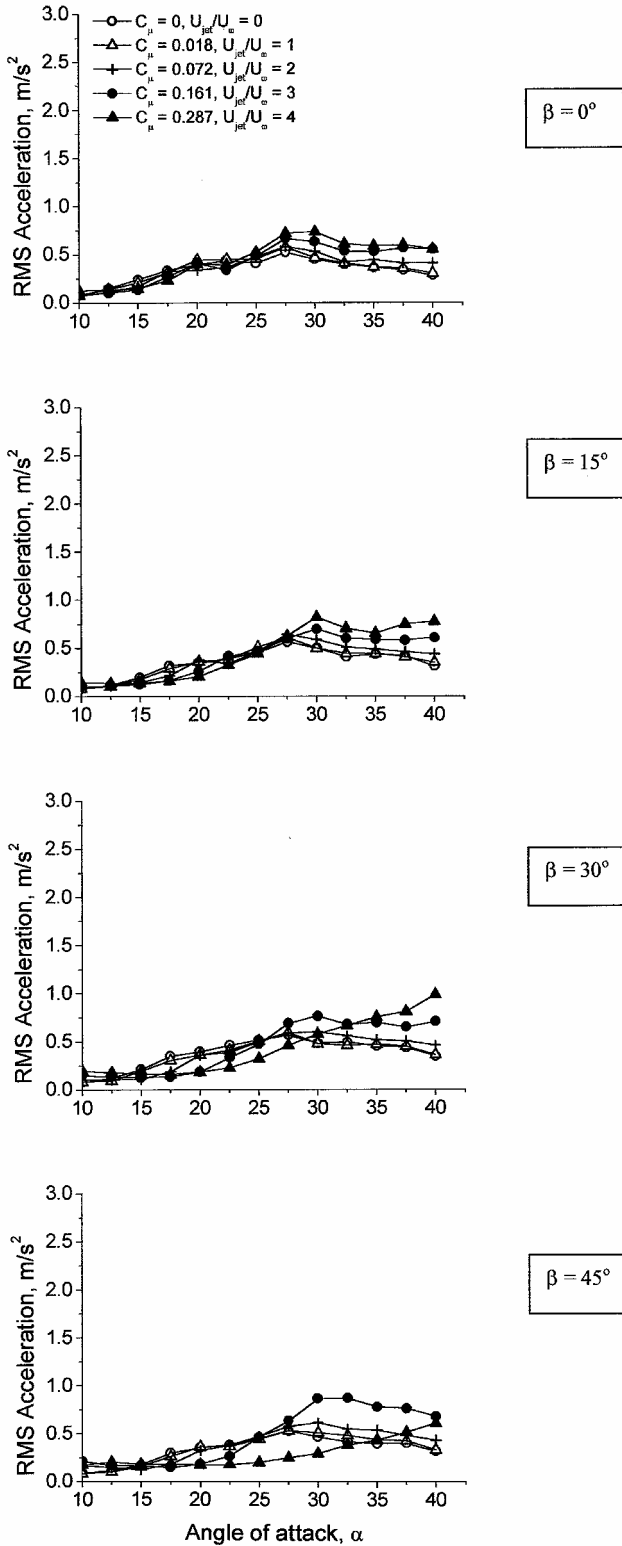


Fig. 15 Variation of rms tip acceleration as a function of incidence for $y_f/s = 0.6$.

for this fin location the spanwise position of the vortex axis coincides with the location of the fin leading edge. For this head-on collision case vortex breakdown is generally upstream of the fin (except for large values of jet momentum coefficient), and the overall level of buffeting is smaller than that of $y_f/s = 0.2$ and 0.4 . It is seen in Fig. 15 that the variation of the rms tip acceleration with angle of attack is also more gradual compared to other cases. The effect of jet blowing at the trailing edge is very small for this fin location for all jet deflection angles tested.

Some experiments were performed in order to study the effect of nozzle geometry. In particular, the nozzle aspect ratio and the nozzle width to wing semispan ratio might be important parameters. The dimensions, width/semispan ratio, and aspect ratio of several nozzles tested are given in Table 1. The original nozzle is denoted as case A in the table. To make a comparison of the effect of nozzle geometry, the momentum coefficient was kept the same for all nozzles tested. The last column in Table 1 shows the velocity ratio U_{jet}/U_∞ for the maximum momentum coefficient used for the original nozzle ($C_\mu = 0.287$). Figure 16 shows the variation of the rms tip

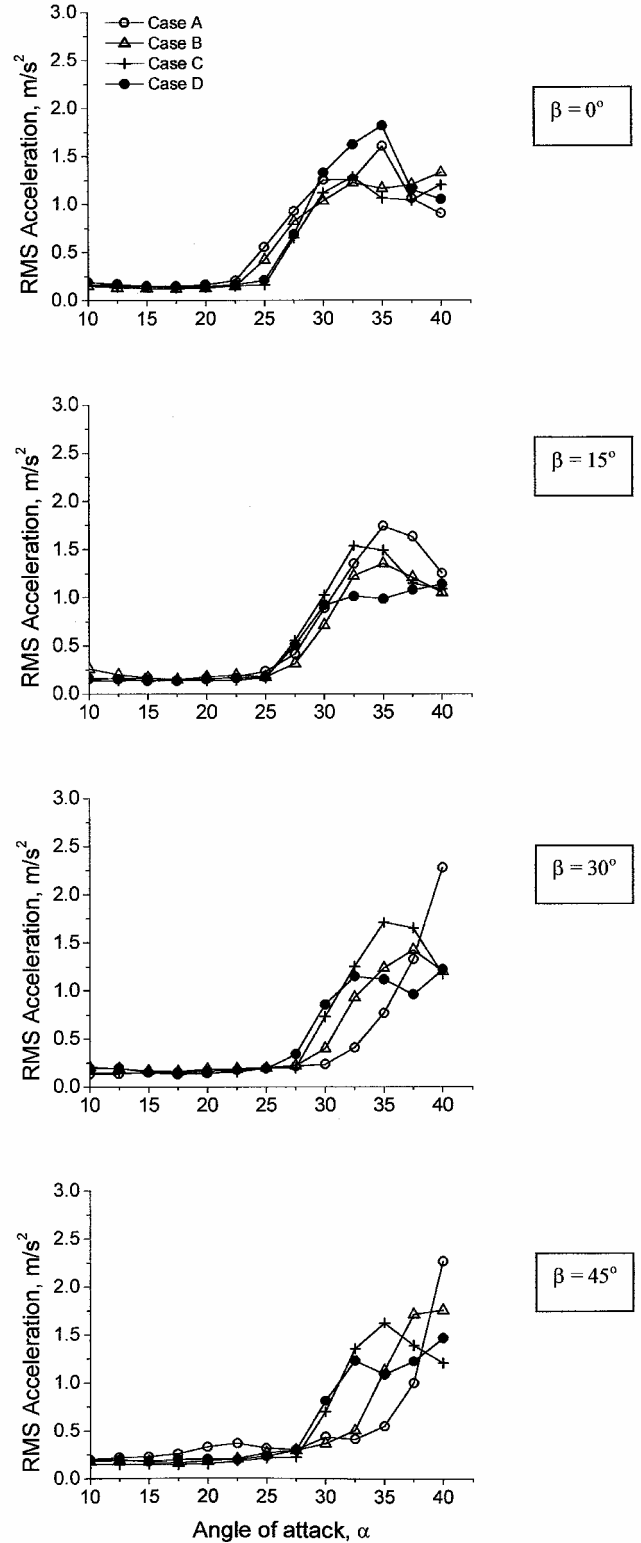


Fig. 16 Variation of rms tip acceleration as a function of incidence for $y_f/s = 0.4$ and $C_\mu = 0.287$.

Table 1 Dimensions, width/semispan, aspect ratio, and velocity ratio for nozzles

Nozzle	Dimensions, mm ²	Width/semispan	Aspect ratio	U_{jet}/U_{∞} ($C_{\mu} = 0.287$)
A	60 × 10	0.45	6	4
B	60 × 5	0.45	12	5.66
C	60 × 2.5	0.45	24	8
D	30 × 5	0.22	6	8

acceleration as a function of angle of attack for four nozzles at various jet deflection angles for $C_{\mu} = 0.287$ and $y_f/s = 0.4$. Buffeting response differs very little for $\beta = 0$ and 15 deg, but there are large effects of nozzle geometry for $\beta = 30$ and 45 deg. At these large deflection angles the original nozzle appears to be more effective in delaying the onset of buffeting, although there is an accompanying increase in the maximum levels of buffeting. Also, although the velocity ratio U_{jet}/U_{∞} is the smallest for the original nozzle (case A, see Table 1) it provides the best performance. In fact, there is a trend

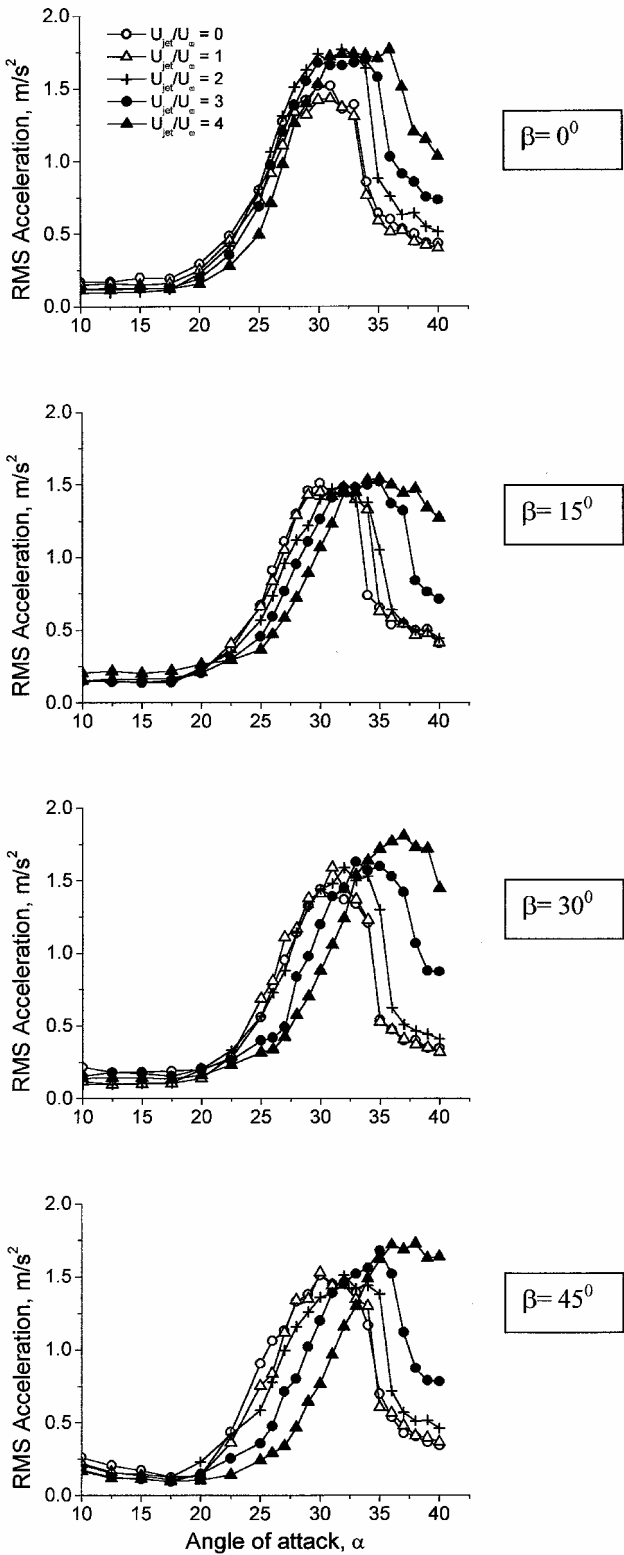


Fig. 17 Variation of rms tip acceleration as a function of incidence for $y_f/s = 0.2$ and $\Lambda = 65$ deg.

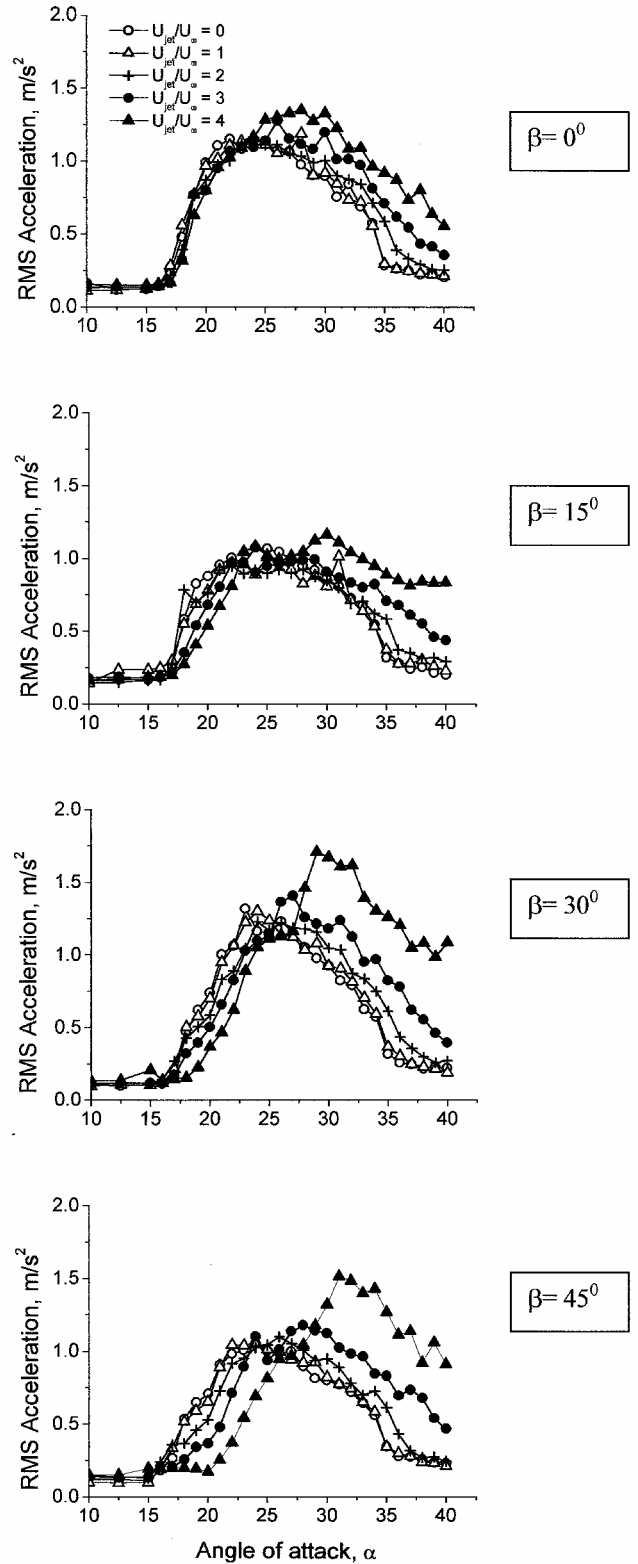


Fig. 18 Variation of rms tip acceleration as a function of incidence for $y_f/s = 0.4$ and $\Lambda = 65$ deg.

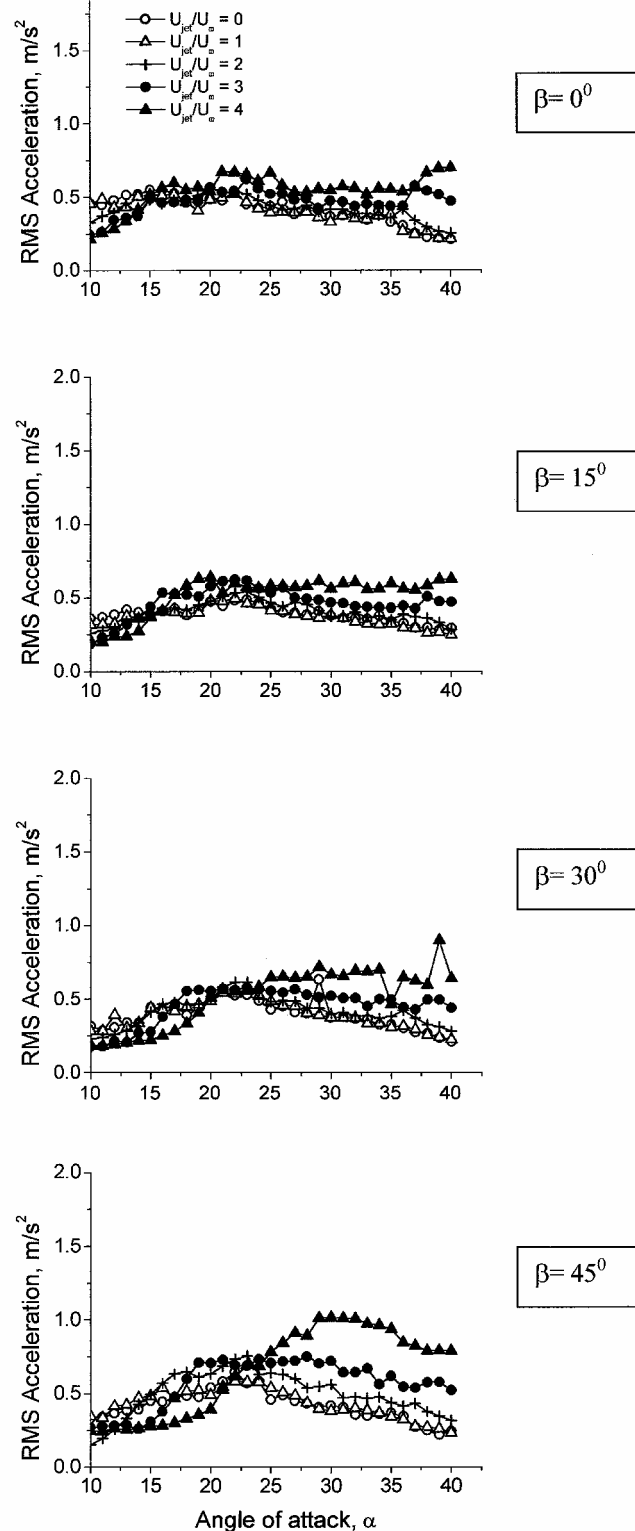


Fig. 19 Variation of rms tip acceleration as a function of incidence for $y_f/s = 0.7$ and $\Lambda = 65$ deg.

that jet blowing becomes less effective with increasing U_{jet}/U_∞ for the constant C_μ . Clearly there remain several aspects of the effect of nozzle geometry to be studied in future work.

Finally, some experiments were carried out to study the effect of wing sweep. One expects that adverse pressure gradient which exists as a result of the trailing edge depends on the slenderness of the wing. With this in mind, detailed experiments were performed for $\Lambda = 65$ deg wing, using the original nozzle. Figures 17–19 show the variation of the rms tip acceleration as a function of angle of attack for various jet velocity ratios; jet deflection angles $\beta = 0$,

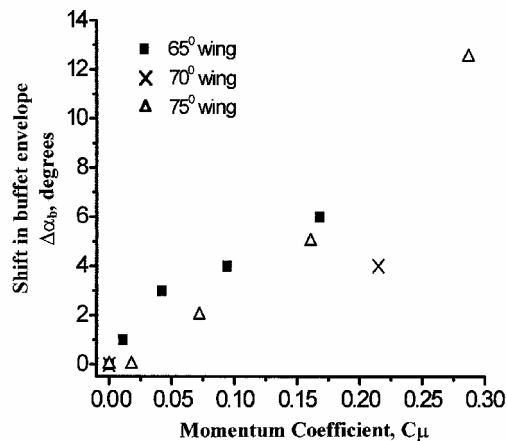


Fig. 20 Maximum shift in incidence in buffet envelope as a function of momentum coefficient for $y_f/s = 0.4$ and $\beta = 45$ deg.

15, 30, 45 deg; and fin locations $y_f/s = 0.2, 0.4,$ and 0.7 (which correspond to head-on collision case for this wing). Note that for the same jet velocity the dimensionless momentum coefficient is smaller for $\Lambda = 65$ -deg wing as a result of larger wing area. Consequently, the maximum momentum coefficient that can be attained is smaller. Nevertheless, the results are qualitatively similar to those obtained for $\Lambda = 75$ deg. Except the head-on collision case, the jet blowing appears to be effective, in particular at higher jet deflection angles. A better comparison for the effect of wing sweep is shown in Fig. 20 for $y_f/s = 0.4$ and $\beta = 45$ deg. Maximum shift in incidence in buffet envelope with respect to $C_\mu = 0$ case is plotted as a function of the momentum coefficient C_μ for all wings. Although there is large scatter in data (presumably because of the effect of nozzle geometry with respect to the wing), the trend confirms that jet blowing is as effective for decreasing wing sweep angle.

Conclusions

Effect of a trailing-edge jet on the interaction of a leading-edge vortex with a fin and resulting fin buffeting was investigated in water tunnel as well as wind-tunnel experiments. Flow visualization studies showed that vortex breakdown is induced as a result of the adverse pressure gradient imposed by the fin, but can be delayed into the wake with increasing jet momentum coefficient. Even for the head-on collision of the leading-edge vortex with the fin, it was possible to eliminate the breakdown completely. Delay of vortex breakdown into the wake even for relatively small values of jet velocity ratio is possible for deflected jets, whereas the effectiveness of the jet with no deflection is very limited. For $\beta = 30$ deg, vortex breakdown can be delayed up to 60% of the chord length depending on the fin location with respect to the leading-edge vortex. Buffeting response of a flexible fin in wind-tunnel experiments showed that the effect of jet momentum was very small for $\beta = 0$ deg, but there was considerable delay of the onset of buffeting to higher angles of attack with increasing jet momentum for $\beta = 30$ and 45 deg. It was found that it was possible to shift the buffeting envelope as much as 12 deg in incidence of the wing. The wind-tunnel tests showed that blowing at the trailing edge appears to be more effective at higher jet deflection angles, which is consistent with the flow visualization results obtained in the water tunnel. It appears that jet blowing is as effective for less slender delta wings.

The results presented in this paper show that vortex breakdown caused by the presence of a fin can be delayed by a trailing-edge jet, with resulting attenuation of fin buffeting. It is suggested that the jet creates a favorable pressure gradient and reduces the adverse pressure gradient caused by the fin. However, there are several factors that need further studies: effect of jet entrainment, vortex interactions between the jet and wing vortices, and the effect of nozzle geometry. Our limited wind-tunnel experiments showed that the nozzle geometry is very important and causes very different buffeting envelopes for the same momentum coefficient.

Acknowledgments

This work was sponsored by the European Office of Aerospace Research and Development, Air Force Office of Scientific Research, USAF, under Contract F61775-01-WE006. The authors acknowledge the help of K. Wong in wind-tunnel experiments.

References

- ¹Gursul, I., and Xie, W., "Buffeting Flows over Delta Wings," *AIAA Journal*, Vol. 37, No. 1, 1999, pp. 58–65.
- ²Triplett, W. E., "Pressure Measurements on Twin Vertical Tails in Buffeting Flow," *Journal of Aircraft*, Vol. 20, No. 11, 1983, pp. 920–925.
- ³Lee, B. H. K., and Brown, D., "Wind-Tunnel Studies of F/A-18 Tail Buffet," *Journal of Aircraft*, Vol. 24, No. 1, 1992, pp. 146–152.
- ⁴Washburn, A. E., Jenkins, L. N., and Ferman, M. A., "Experimental Investigation of Vortex-Fin Interaction," AIAA Paper 93-0050, Jan. 1993.
- ⁵Meyn, L. A., and James, K. D., "Full Scale Wind Tunnel Studies of F/A-18 Tail Buffet," AIAA Paper 93-3519, 1993.
- ⁶Lee, B. H. K., and Tang, F. C., "Characteristics of the Surface Pressures on a F/A-18 Vertical Fin due to Buffet," *Journal of Aircraft*, Vol. 31, No. 1, 1994, pp. 228–235.
- ⁷Bean, D. E., and Wood, N. J., "Experimental Investigation of Twin-Fin Buffeting and Suppression," *Journal of Aircraft*, Vol. 33, No. 4, 1996, pp. 761–767.
- ⁸Wolfe, S., Canbazoglu, S., Lin, J. C., and Rockwell, D., "Buffeting of Fins: An Assessment of Surface Pressure Loading," *AIAA Journal*, Vol. 33, No. 11, 1995, pp. 2232–2234.
- ⁹Mayori, A., and Rockwell, D., "Interaction of a Streamwise Vortex with a Thin Plate: A Source of Turbulent Buffeting," *AIAA Journal*, Vol. 32, No. 10, 1994, pp. 2022–2029.
- ¹⁰Wolfe, S., Lin, J. C., and Rockwell, D., "Buffeting at the Leading-Edge of a Flat Plate due to a Streamwise Vortex: Flow Structure and Surface Pressure Loading," *Journal of Fluids and Structures*, Vol. 9, No. 4, 1995, pp. 359–370.
- ¹¹Canbazoglu, S., Lin, J. C., Wolfe, S., and Rockwell, D., "Buffeting of Fins: Distortion of Incident Vortex," *AIAA Journal*, Vol. 33, No. 11, 1995, pp. 2144–2150.
- ¹²Gordnier, R. E., and Visbal, M. R., "Numerical Simulation of the Impingement of a Streamwise Vortex on a Plate," AIAA Paper 97-1781, June–July 1997.
- ¹³Gursul, I., and Xie, W., "Interaction of Vortex Breakdown with an Oscillating Fin," *AIAA Journal*, Vol. 39, No. 3, 2001, pp. 438–446.
- ¹⁴Hauch, R. M., Jacobs, J. H., Dima, C., and Ravindra, K., "Reduction of Vertical Tail Buffet Response Using Active Control," *Journal of Aircraft*, Vol. 33, No. 3, 1996, pp. 617–622.
- ¹⁵Breitsamter, C., and Laschka, B., "Aerodynamic Active Control for EF-2000 Fin Buffet Load Alleviation," AIAA Paper 2000-0656, Jan. 2000.
- ¹⁶Bean, D. E., Greenwell, D. I., and Wood, N. J., "Vortex Control Technique for the Attenuation of Fin Buffet," *Journal of Aircraft*, Vol. 30, No. 6, 1993, pp. 847–853.
- ¹⁷McCormick, S., and Gursul, I., "Effect of Shear Layer Control on Leading-Edge Vortices," *Journal of Aircraft*, Vol. 33, No. 6, 1996, pp. 1087–1093.
- ¹⁸Gursul, I., Srinivas, S., and Batta, G., "Active Control of Vortex Breakdown over a Delta Wing," *AIAA Journal*, Vol. 33, No. 9, 1995, pp. 1743–1745.
- ¹⁹Mitchell, A. M., and Delery, J., "Research into Vortex Breakdown Control," *Progress in Aerospace Sciences*, Vol. 37, 2001, pp. 385–418.
- ²⁰Helin, H. E., and Watry, C. W., "Effects of Trailing-Edge Jet Entrainment on Delta Wing Vortices," *AIAA Journal*, Vol. 32, No. 4, 1994, pp. 802–804.
- ²¹Shih, C., and Ding, Z., "Trailing-Edge Jet Control of Leading-Edge Vortices of a Delta Wing," *AIAA Journal*, Vol. 34, No. 7, 1996, pp. 1447–1457.
- ²²Vorobieff, P. V., and Rockwell, D. O., "Vortex Breakdown on Pitching Delta Wing: Control by Intermittent Trailing-Edge Blowing," *AIAA Journal*, Vol. 36, No. 4, 1998, pp. 585–589.
- ²³Mitchell, A. M., Molton, P., Barberis, D., and Delery, J., "Control of Leading-Edge Vortex Breakdown by Trailing Edge Injection," AIAA Paper 99-3202, 1999.
- ²⁴Ross, H., "X-31, The First Aircraft Designed for High Angle of Attack Manoeuvring," NATO AVT Meeting, May 2001.
- ²⁵Lambert, C., and Gursul, I., "Buffeting of a Flexible Fin over a Delta Wing," AIAA Paper 2001-2426, June 2001.
- ²⁶Lambourne, N. C., and Bryer, D. W., "The Bursting of Leading Edge Vortices—Some Observations and Discussion of the Phenomenon," Aeronautical Research Council, R&M 3282, London, April 1961.
- ²⁷Wang, F. Y., Proot, M. M. J., Charbonnier, J. M., and Sforza, P. M., "Near-Field Interaction of a Jet with Leading-Edge Vortices," *Journal of Aircraft*, Vol. 37, No. 5, 2000, pp. 779–785.